A NOTE ON PLANAR HEXAGONAL MESHES

WENPING WANG * YANG LIU *

Abstract. We study the geometry and computation of free-form hexagonal meshes with planar faces (to be called *P-Hex meshes*). Several existing methods are reviewed and a new method is proposed for computing P-Hex meshes to approximate a given surface. The outstanding issues with these methods and further research directions are discussed.

Key words. planar hexagonal meshes, Dupin indicatrix, polyhedral approximation.

1. Introduction. A hexagonal mesh with planar faces is a discrete polyhedral surface in 3D whose faces are planar hexagons and whose vertices have degree 3. It will be abbreviated as the *P-Hex mesh* through out this paper. P-Hex meshes are used in architecture design of glass/steel panel structures and provide a useful representation for various special surfaces, such as minimal surfaces or constant mean curvature surfaces [2], in discrete differential geometry. (See Figure 1.) There are several existing methods for computing a P-Hex mesh to approximate a given shape. We will review these methods to motivate further research. In addition, we will study the geometric properties of P-Hex meshes and present a new method for computing P-Hex meshes. We will consider robust computation of offset surfaces specific to P-Hex meshes.

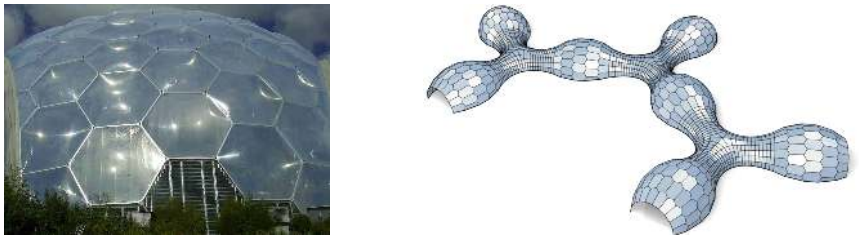

FIG. 1. *Left: A geodome constructed using a P-Hex mesh in the Eden Project in UK; right: the convex parts of this model are constant mean curvature (CMC) surfaces modeled by P-Hex meshes [6].*

The requirement on face planarity of P-Hex meshes arises naturally in modeling of glass/steel panel structures in architecture. Each flat glass panel, represented by a hexagonal face, is framed by beams which are joined at nodes represented by the vertices of the mesh. The node complexity, defined as the number of beams joined at a node, is a major consideration in manufacturing cost. Since their vertices have degree 3, the

*Department of Computer Science, University of Hong Kong, Pokfulam Road, Hong Kong SAR, P.R. China. The work was partially supported by the National Key Basic Research Project of China under 2004CB318000.

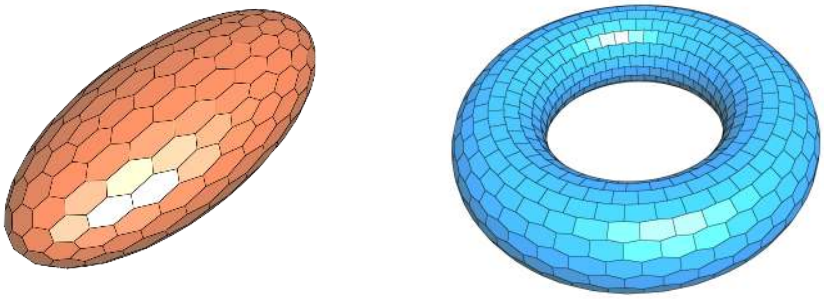

FIG. 2. *Left: An ellipsoid tiled with P-Hex faces and 12 planar pentagons; right: a torus tiled entirely with P-Hex faces.*

P-Hex meshes offer the simplest node complexity compared with meshes with planar quadrilateral faces or triangle meshes [6].

Only a closed surface of genus 1 (e.g. a torus) may be tiled with a P-Hex mesh. On a closed surface of genus 0, faces other than hexagons must be used, provided that all the vertices are of degree 3 (for example, see Figure 2). Assuming that only hexagons and pentagons are allowed, it is easy to show that there have to be exactly 12 pentagons. A typical soccer ball is an example of such a tiling of a surface of genus 0, which has 12 pentagons and 20 hexagons.

Two concepts important to the study of P-Hex meshes are *conjugate curve network* and the *Dupin indicatrix* of a surface. Consider a point p on a surface S. Let $T_p(S)$ denote the 2D space of tangent vectors to S at p. Then the differential of the Gauss map, which is the differential $\mathrm{d}N$ of the unit normal vector N of S at p, defines a self-adjoint linear map on $T_p(S)$. Two vectors v and w are *conjugate* at p if the inner product $\langle \mathrm{d}N(v), w\rangle = 0$ [7]; note that this relationship is symmetric, since $\mathrm{d}N$ is a self-adjoint. In particular, at a point p on a developable surface the unique ruling direction at p is conjugate to any other direction. A *conjugate curve network* on S consists of two families of curves, F_1 and F_2, on S such that at any point $p \in S$ there is a unique curve in F_1 and a unique curve in F_2 passing through p and the tangent vector to the curve in F_1 and the tangent vector to the curve in F_2 are conjugate.

Suppose that we have a 2D local coordinate system on $T_p(S)$ with the x and y axes aligned with the principal curvature directions of S at p. Then the *Dupin indicatrix* is a conic defined by $\kappa_1 x^2 + \kappa_2 y^2 = \pm 1$, where κ_1, κ_2 are principal curvatures [7]. Specifically, when p is an elliptic point, assuming that the two principal curvatures $\kappa_1 > 0$ and $\kappa_2 > 0$ by changing the orientation of the surface if necessary, the Dupin indicatrix is the ellipse $\kappa_1 x^2 + \kappa_2 y^2 = 1$. When p is a hyperbolic point, the Dupin indicatrix consists of two hyperbolas $\kappa_1 x^2 + \kappa_2 y^2 = \pm 1$ having the same

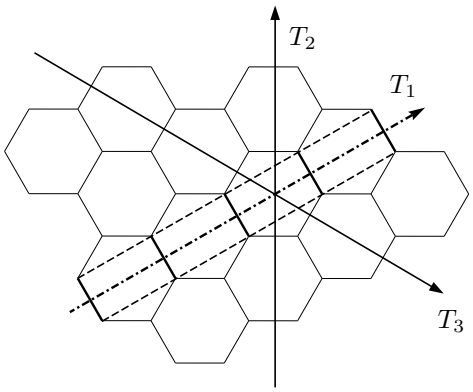

FIG. 3. *Three strips on a P-Hex mesh along the directions T_1, T_2 and T_3.*

pair of asymptotic lines. When p is a parabolic point, assuming that $\kappa_1 \neq 0$ and $\kappa_2 = 0$, the Dupin indicatrix is the pair of lines $\kappa_1 x^2 = \pm 1$. The Dupin indicatrix is not defined at a planar point, where $\kappa_1 = \kappa_2 = 0$. Within the above 2D x-y coordinate system in $T_p(S)$, the Dupin indicatrix has the polar representation $\rho = \pm 1/\sqrt{|\kappa(\theta)|}$, where $\kappa(\theta)$ is the normal curvature of S in the direction of the vector $(\cos\theta, \sin\theta)^T$.

We will take an asymptotic approach in our subsequent analysis. We assume a sequence of P-Hex meshes converging to a surface S, with each hex face h converging to the tangent plane of S at the center of h. An asymptotic analysis is useful to designing numerical methods in practice when a P-Hex mesh is a close approximation to a smooth surface and the faces of the P-Hex meshes are sufficiently small.

A P-Hex mesh comprises three families of developable strips (see Figure 3). Here a developable strip is a surface consisting of a sequence of planar faces joining consecutively along line segments. A developable trip has a central curve formed by the polygon connecting the centers of consecutive hex faces of the strip. Note that the edges between consecutive faces of a developable strip are the discrete rulings of the developable strip. Therefore these edges are conjugate to the direction of the central curve, as a consequence of the discrete analogue of the class result for smooth developable surfaces [7].

At the center of a hex face h, the central curves of the three strips containing h define three directions. Meanwhile, we assume that in the limit each pair of opposite edges of h are parallel, that is, h has central symmetry. Therefore, the three pairs of opposite edges of h define another three directions at the center of h. It follows that the first three directions are conjugate to the latter three, respectively. Hence, the hex face is constrained by a homothetic copy of the Dupin indicatrix, as summarized by the following theorem. (A *homothetic copy* of a shape is the image of the

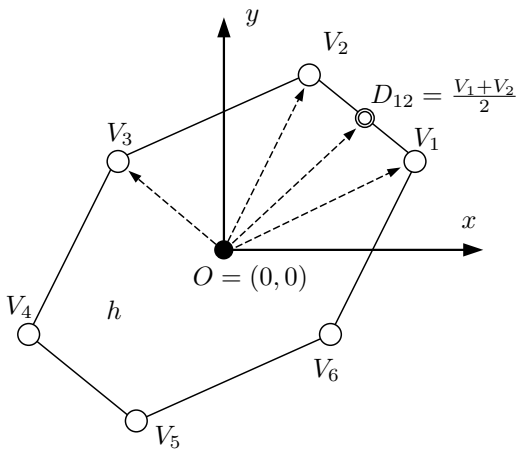

FIG. 4. *Illustration for the proof of Theorem 1.*

shape under uniform scaling and translation.)

Theorem 1: *Let M be a P-Hex mesh converging to a surface S, with each face of M converging to the tangent plane of S at the center of the face. Let h be a face of M with its center being a point O on the surface S. In the limit, h is inscribed to a homothetic copy of the Dupin indicatrix of the surface S at O.*

PROOF: Refer to Figure 4. First we set up a local 2D coordinate system on the tangent plane Γ of the surface $\mathcal{S}$ at O, with the coordinate axes in the principal curvature directions at O. In the limit we can assume that h lies on the tangent plane Γ, with its center at O. Due to its central symmetry, the hex face h is uniquely determined by its vertex vectors V_1, V_2, V_3, with $V_4 = -V_1$, $V_5 = -V_2$, and $V_6 = -V_3$.

In the above 2D coordinate system on the tangent plane Γ, denote $V_i = (\ell_i \cos\theta_i, \ell_i \sin\theta_i)^T$, $i = 1, 2, 3$, subject to that $\ell_i > 0$, $\theta_1 < \theta_2 < \theta_3$ and $\theta_3 - \theta_1 < \pi$. Consider any two consecutive vertices, say V_1 and V_2 (Figure 4). Note that the strip along the central curve direction $D_{12} = (V_1 + V_2)/2$ is conjugate to the ruling direction $V_2 - V_1$ with respect to the inner product $\langle X, Y\rangle \equiv X^T \mathrm{diag}(\kappa_1, \kappa_2) Y$ defined by the second fundamental form. Therefore,

$$\kappa_1(\ell_1^2 \cos^2\theta_1 - \ell_2^2 \cos^2\theta_2) + \kappa_2(\ell_1^2 \sin^2\theta_1 - \ell_2^2 \sin^2\theta_2) = 0.$$

It then follows from Euler's theorem that

$$\kappa(\theta_1)\ell_1^2 - \kappa(\theta_2)\ell_2^2 = 0, \tag{1.1}$$

where $\kappa(\theta_j)$ is the normal curvature in the direction $(\cos\theta_j, \sin\theta_j)^T$, $j = 1, 2$. Comparing (1.1) with the polar representation of the Dupin indicatrix given previously, we conclude that the six vertices of h lie on a homothetic copy of the Dupin indicatrix. □

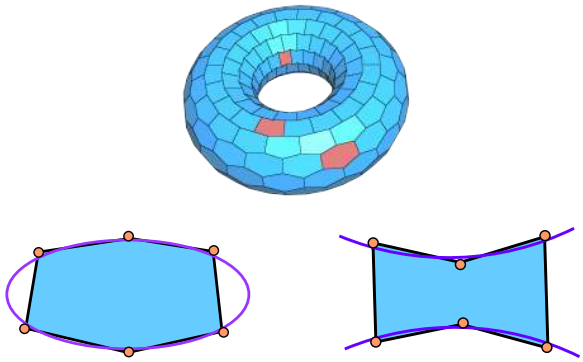

FIG. 5. *Upper: A P-Hex mesh tiling a torus; lower left: a convex P-Hex face is in a first approximation inscribed to a homothetic copy of the Dupin conic, which is an ellipse, when $K > 0$; lower right: a concave P-Hex face is in a first approximation inscribed to a homothetic copy of the Dupin conic, which is a hyperbola, when $K < 0$.*

The above analysis indicates that convex planar hex faces appear only in an elliptic region of a surface, where the Gaussian curvature $K > 0$ and the Dupin indicatrix is an ellipse, and the P-Hex faces are concave hexagons in a hyperbolic region, where $K < 0$, since they are inscribed to hyperbolas (see Figure 5). Even in an elliptic region, we in general cannot expect to have P-Hex faces to be regular hexagons, since the Dupin indicatrix is in general not a circle.

2. Existing Methods. In [3] stereographic projection is used to map a power diagram of a set of points in 2D, which is an extension of Voronoi diagram, onto an ellipsoid to form a polyhedral surface with planar faces. If the faces of the power diagram are hexagons, then a P-Hex mesh approximating the ellipsoid will be generated. This method cannot be extended to other types of quadrics, such as a hyperboloid of one-sheet, or more general free-form surfaces.

An elegant and effective approach to computing a P-Hex mesh is based on projective duality, which establishes a relationship between a triangular mesh and a P-Hex mesh. In fact, this relationship has been used to derive subdivision rules for P-Hex meshes from subdivision rules for triangle meshes [4]. When applying this approach to generating a P-Hex mesh from a triangle mesh, it suffers from the lack of robustness common to several other existing methods.

Recall that projective duality is a transformation that maps a plane $aX + bY + cZ + dW = 0$ in 3D prime space into the point $Q(X, Y, Z, W)^T$ in homogenous coordinates in dual space, where Q is a given symmetric matrix. With an affine specialization, we consider the particular duality that maps a plane not passing through the origin, in the form $ax + by +$

$cz + 1 = 0$ in primal space, to a point $(a, b, c)^T$ in dual space. Under this mapping, a surface S is mapped to another surface S', called the *dual* of S, consisting of points corresponding to the tangent planes of S. Clearly, a P-hex mesh approximating a surface S is dual to a regular triangle mesh approximating S', the dual of S, with each hex face being dual to a degree 6 vertex of the triangle mesh. This property suggests the following method for computing a P-Hex mesh. Given a surface S, first compute the dual S' of S, then compute a regular triangulation of S', and finally map this triangulation to a P-Hex mesh approximating S.

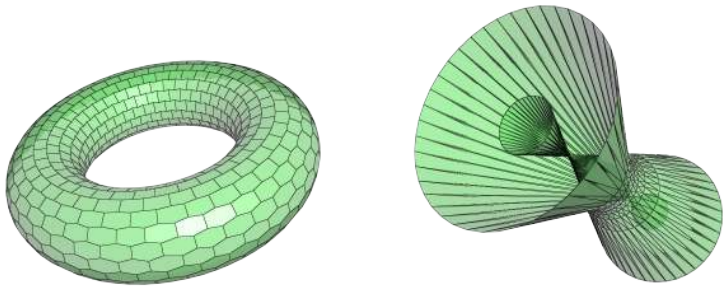

FIG. 6. *Left: a P-Hex mesh approximating a torus; right: the projective dual of the torus with its triangulation corresponding to the P-Hex mesh in the left figure.*

However, there are three major problems with this approach: 1) projective duality may have high metric distortion and parabolic points of S give rise to singular points on S' (see Figure 6). These make it difficult to compute a good triangle mesh on S'; 2) Under projective duality the correspondence between the points of S and the points of S' is often not one-to-one. This makes it difficult to map a triangulation of S' in dual space back to a P-Hex mesh of S in primal space; 3) It is not clear what kind of triangle meshes of S' correspond to P-Hex meshes whose faces are free of self-intersection (see Figure 7). As the consequence of these drawbacks, the method based on projective duality cannot be used to generate P-Hex mesh tiling a free-form surface S. Moreover, even when S is convex the method often generates invalid P-Hex meshes with self-intersecting faces, as illustrated in Figure 7.

The method in [1] uses the supporting function defined over the Gaussian sphere of a free-form surface S to compute a P-Hex mesh. The idea is to first obtain a piecewise linear approximation of the supporting function over a triangulation of the Gaussian sphere. Then it can be shown that the surface determined by this piecewise linear supporting function is a P-Hex mesh approximating the surface S.

Consider a tangent plane $ax + by + cz + 1 = 0$ of S. With the support function, this tangent plane is represented by the unit normal vector $(a/m, b/m, c/m) \in S^2$, where $m = (a^2 + b^2 + c^2)^{1/2}$, and its dis-

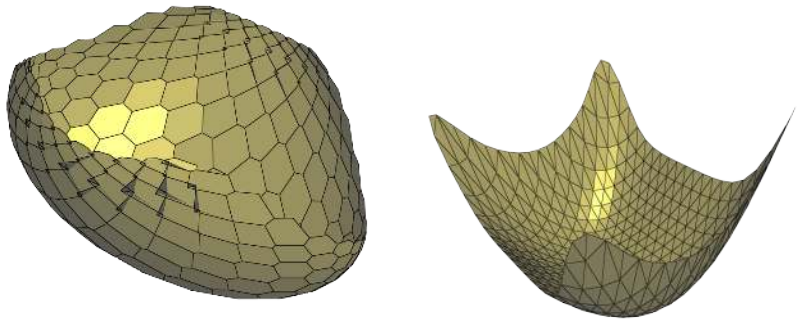

FIG. 7. *Left: a convex surface S approximated by a self-intersecting P-Hex mesh; right: The dual of S represented by a triangular mesh corresponding to the P-Hex mesh in the left figure.*

tance from the origin $(0, 0, 0)$ to the plane, which is $1/m$. Therefore, the graph of the support function over S^2 can be represented by the point $\mathbf{p} = \frac{1}{m}(a/m, b/m, c/m) = (a/m^2, b/m^2, c/m^2)$. We recognize that $\mathbf{p}$ is the inversion with respect to the sphere S^2 of the point $(a, b, c)^T$, which is the dual point of the tangent plane $ax + by + cz + 1 = 0$. Hence, the support function can be regarded as the composition of the duality and the spherical inversion with respect to S^2. Because of this, the method in [1] has the same limitations of the other methods based on projective duality. As a consequence, it can only be applied to a surface patch with all elliptic points ($K > 0$) or all hyperbolic points ($K < 0$), and even in these simple cases it often produces invalid P-Hex meshes.

The concept of *parallel meshes* is proposed in [6] for defining and computing various types of offset surfaces of a mesh surface. It may also be used for computing P-Hex mesh for simple surfaces, such as a surface patch with $K > 0$ everywhere or $K < 0$ everywhere. With this method, for example, the convex parts of the model in Figure 1(b) are modeled as P-Hex meshes parallel to a convex Koebe mesh [6]. A restrictive assumption here is that there is already a P-Hex mesh H available, and a new P-Hex mesh H' approximating a given surface S will then be generated as a parallel mesh of H. Moreover, again in this case the P-Hex mesh H' often contains faces with self-intersection.

This review shows that no existing method is capable of computing a valid P-Hex mesh of free-form shape. So it will be a breakthrough if a robust method can be developed for computing valid free-form P-Hex meshes. There are two major problems we must address to achieve this goal. The first is *generality* — we hope to have a method capable of computing a P-Hex surface approximating any free-form surface, with elliptic,

hyperbolic, and parabolic regions all existing on the same surface. The second is *validity* — as the most basic requirement by practical applications, we need to ensure that the faces of the computed P-Hex mesh are free of self-intersection. In addition, from the design point of view, there is a need to explore the full flexibility of P-Hex meshes to allow fine control of the shape and size of the hexagonal faces of a P-Hex mesh.

3. A New Method. We will propose a simple method for computing P-Hex meshes. This method has two main steps – we first compute an initial hexagonal mesh that is close to a P-Hex mesh and then use local perturbation to produce the final P-Hex mesh.

As input we start with a conjugate curve network on a target surface S to be approximated (see the left figure of Fig. 8). Sampling these two families of curves, we obtain a quad mesh that is nearly a planar quad mesh [5]. Then we shift every other row of the quad mesh to form a brick-wall layout, which consists of nearly planar hexagonal faces. (See the middle figure of Fig. 8).

In the second step we use nonlinear optimization to locally perturb the above hexagonal mesh into an exact P-Hex mesh. Note that every 4-point subset of the 6 vertices of a hex face defines a tetrahedron. Obviously, the hex face is planar if and only if the volumes of all these tetrahedra are zero. Therefore, the constraints of our optimization are that the volumes of all the tetrahedra of all the hex faces be zero. To prevent the vertices of the hex mesh from shifting away from the target surface S, we minimize an objective function defined as the sum of the squared distances of the mesh vertices to S. Thus, we end up with a constrained nonlinear least squares problem. We have implemented a penalty method to solve this problem and obtained satisfactory results. The flow of processing is illustrated using a torus in Figure 8. Figure 9 shows the computation of a P-Hex mesh approximating an open surface patch containing different types of curved regions.

The new method can handle a general surface which contains both regions of positive curvature and regions of negative curvature. Empirically, the face self-intersection are removed by using appropriate sampling sizes of the input conjugate curve network. However, a clear theoretical understanding of face self-intersection and a guaranteed practical measure for avoiding it are still missing. We also need to point out that the new method only produces approximately planar hexagonal faces due to its minimization nature, while previously duality-based methods produce exactly planar hexagonal faces.

4. Offset Mesh. A closely related issue is the computation of the offset surfaces of P-Hex meshes, which are demanded for modeling multi-layered supporting structures of a glass panel structure. The offset of a polyhedral surface is the discrete analogue of the offset surface of a smooth surface. There are several variants of the offset of a polyhedral surface; the

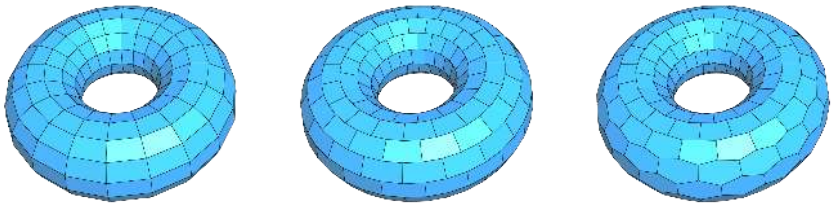

FIG. 8. *Left: a conjugate curve network; middle: the hexagonal mesh obtained by "shifting" alternative rows of the network in the left figure; right: a P-Hex mesh obtained by locally perturbing the hexagonal mesh in the middle figure.*

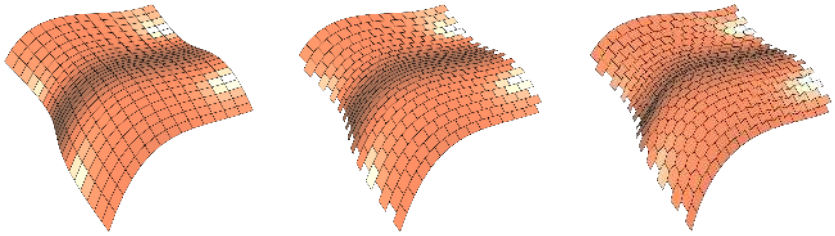

FIG. 9. *Computation of a P-Hex mesh approximating an open surface. Left: a conjugate curve network; middle: the intermediate hexagonal mesh; right: the final P-Hex mesh after local perturbation.*

most obvious one is the *constant-face-distance offset*, which is a polyhedral surface obtained by displacing each face of a given polyhedral surface by a constant distance along the normal of the face. In the following, a polyhedral surface will also be called a mesh, with the understanding that each face of the mesh is a planar polygon.

The offset mesh is closely related to the notion of *parallel meshes* — two meshes are *parallel* to each other if they are isomorphic and their corresponding edges have non-zero lengths and are parallel to each other. According to [6], the constant-distance offset of a smooth surface can be extended to the setting of polyhedral surfaces in three different ways: (1) constant face-distance offset; (2) constant edge-distance offset; and (3) constant vertex-distance offset. In terms of parallel meshes, a mesh M possesses a constant face-distance offset if it has a parallel mesh M' whose faces are tangent to S^2; a mesh M possesses a constant edge-distance offset if it has a parallel mesh M' whose edges are tangent to S^2; and a mesh M possesses a constant vertex-distance offset if it has a parallel mesh M' whose vertices are on S^2. In the three cases above, the parallel mesh M' is called the *discrete Gaussian image* of the given mesh M. Then an offset mesh M_d with offset distance d of the mesh M is given by $M_d = M + d \cdot M'$, which is understood to be a vector expression for the corresponding ver-

tices of the three meshes M, M' and M_d. We refer the reader to [6] for more detailed discussions about the definition, existence and construction of offset of general polyhedral surfaces.

In the following we will consider computing the offset meshes of P-Hex meshes. An equivalent condition for a mesh M with planar faces to possess a face-distance offset is that for every vertex v of M, all the faces incident to v are tangent to a common cone of revolution. For this reason, a mesh M possessing this property is also called a *conical mesh*. Obviously, this condition is satisfied by any P-Hex mesh, since there are exactly three faces incident to any vertex of a P-Hex mesh. That is, any P-Hex mesh is a conical mesh; as a consequence, any P-Hex mesh possesses constant face-distance offset P-Hex meshes.

Given a P-Hex mesh, its offset with the face-distance equal to a constant d can be computed as follows. For each vertex, we offset the three incident faces outward along their face normals by the distance d and intersect the three planes containing the three offset faces to determine the vertex of the offset mesh. Clearly, this approach will fail when the three faces are co-planar and it is numerically unstable when the three faces are nearly co-planar.

A more robust scheme is as follows. Let f_i, $i = 0, 1, 2$, be the three hex faces incident to a vertex v of a P-Hex mesh M. Let v_d be the vertex of the offset mesh M_d corresponding to v. Let N_i denote unit normal vectors of the f_i. Let θ_i be the internal angle of f_i at v. Then the "vertex" normal vector N_v of M ar v, defined by $v_d - v$, is parallel to

$$\bar{N}_v = \sum_{i=0}^{2} (\tan\beta_i + \tan\gamma_i) N_i,$$

where $\beta_i = \frac{1}{2}(\theta_i + \theta_{i+1} - \theta_{i-1})$ and $\gamma_i = \frac{1}{2}(\theta_i + \theta_{i-1} - \theta_{i+1})$, $i = 0, 1, 2$, mod 3. The proof of this formula is elementary so we omit it here. Using this formula, the vertex v_d can be determined by intersecting the line $p(t) = v + t\bar{N}_v$ with any one of the offset planes of the three faces. Figure 10 shows a P-Hex mesh with its constant face-distance offset mesh.

Next we consider the constant vertex-distance offset of a P-Hex mesh. An arbitrary P-Hex mesh may not possess a constant vertex-distance offset mesh. According to the above discussion, a necessary and sufficient condition for a P-Hex mesh M to have a constance vertex-distance offset is that it is parallel to a P-Hex mesh M' inscribed to the sphere S^2. Clearly, if there is such a mesh M', then every hex face of M' is inscribed to a circle. Let h' be a face of M'. Let α'_i, $i = 0, 1, \ldots, 5$, denote the six consecutively ordered internal angles of h' (see Figure 11). Then, since h' is inscribed to a circle, it is easy to show that $\alpha'_0 + \alpha'_2 + \alpha'_4 = \alpha'_1 + \alpha'_3 + \alpha'_5$. Let h be the hex face of M corresponding to h'. Let the α_i, $i = 0, 1, \ldots, 5$, be the corresponding angles of h. Since the edges of the face h are parallel to the edges of the face h' of M', $\alpha_i = \alpha'_i$. Therefore $\alpha_0 + \alpha_2 + \alpha_4 = \alpha_1 + \alpha_3 + \alpha_5$.

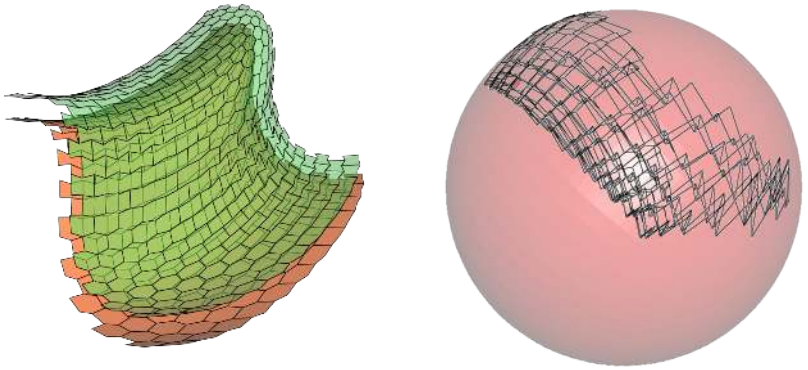

FIG. 10. *Left: A free-form P-Hex mesh and its constant face-distance offset mesh; right: the Gauss image of the P-Hex mesh, whose faces are tangent to the sphere* S^2.

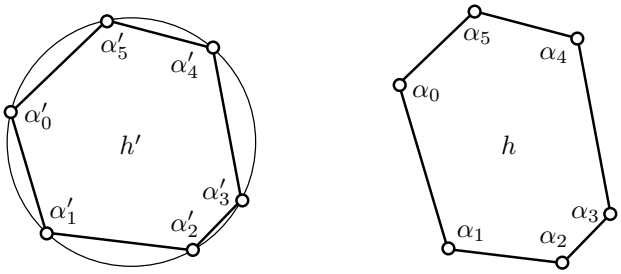

FIG. 11. *Left: A hex face* h' *inscribed to a circle; right: a hex face* h *parallel to* h'.

Conversely, it is easy to see that if

$$\alpha_0 + \alpha_2 + \alpha_4 = \alpha_1 + \alpha_3 + \alpha_5 \tag{4.1}$$

for a planar hex face h, then h is parallel to a hex face h' that is inscribed to a circle. From this it can be shown that, for an open P-Hex mesh M surface, it possesses a constant vertex distance offset mesh if and only if the angle condition (4.1) holds for every hex face h of M. That is to say, the angle condition (4.1) is a necessary and sufficient condition for a P-Hex mesh to possess constant vertex-distance offset meshes. Note that this angle condition (4.1) is only a necessary condition on this existence of constant vertex-distance offset meshes of a P-Hex mesh of a more complex topological type.

Figure 12 shows a P-Hex mesh whose faces satisfy the angle condition (4.1), together with its constant vertex-distance offset mesh, computed by integrating the angle condition (4.1) as a constraint in our local perturbation method.

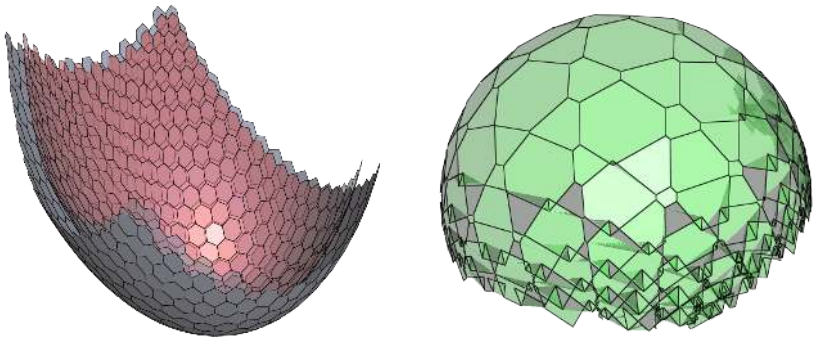

FIG. 12. *Left: A P-Hex satisfying the angle condition given by Eqn. (4.1), with its constant vertex-distance offset P-Hex mesh (superimposed); right: the Gauss image of the P-hex mesh, whose vertices are on the sphere* S^2.

According to [6], a P-Hex mesh possessing a constant edge-distance offset is necessarily parallel to a Koebe mesh, a mesh whose edges are tangent to the unit sphere S^2. This imposes significant restriction to the kind of surface shapes that can be represented by such P-Hex meshes. Also, the computation of the constant edge-distance offset meshes is more involved than the other types. For the detail we refer the reader to [6].

5. Further Problems. There are numerous open problems calling for further research. First, it is important to understand the inherent degrees of freedom of P-Hex meshes tiling a free form surface. Such an understanding is fundamental to developing a general method for computing P-Hex meshes. Second, the issue of avoiding face self-intersection of P-Hex faces is still outstanding. All the existing methods, as well as the new method we have proposed here, cannot ensure that the computed P-Hex mesh is free of face self-intersection. We refer the reader to our recent technical report [8] on yet another method for generating P-Hex meshes based on tangent-duality and characterization of non-self-intersecting P-Hex faces in that context.

In view of practical applications in shape design, it would be desirable to be able to exert fine control over the the shape and size of the faces of a P-Hex mesh. Also, a subdivision scheme for P-Hex meshes would be very useful design tool. Finally, more research is needed on the computation of offset meshes of P-Hex meshes, especially in the case of constant edge-distance offset meshes.

6. Acknowledgments. This research is supported by a General Research Fund (717808E) of Hong Kong Research Grant Council. The authors would like to thank Prof. Helmut Pottmann and Prof. Johannes Wallner for helpful discussions.

REFERENCES

[1] H. Almegaard, A. Bagger, J. Gravesen, B. Jüttler, and Z. Sir, *Surfaces with piecewise linear support functions over spherical triangulations*, in Proceedings of Mathematics of Surfaces XII, LNCS 4647, Springer, 2007.

[2] A. Bobenko, T. Hoffmann, and B. Springborn, *Minimal surfaces from circle patterns: Geometry from combinatorics*, Ann. of Math., vol. 164, pp. 231–264, 2006.

[3] J. Díaz, C. Otero, R. Togores, and C. Manchado, *Power diagrams in the design of chordal space structures*, in The 2nd International Symposium on Voronoi Diagrams in Science and Engineering, pp. 93–104, 2005.

[4] H. Kawaharada and K. Sugihara, *Dual subdivision - a new class of subdivision schemes using projective duality*, in The 14th International Conference in Central Europe on Computer Graphics, Visualization and Computer Vision, pp. 9–17, 2006.

[5] Y. Liu, H. Pottmann, J. Wallner, Y. Yang, and W. Wang, *Geometric modeling with conical meshes and developable surfaces*, ACM Transactions on Graphics (SIGGRAPH 2006), 25(3), pp. 681–689, 2006.

[6] H. Pottmann, Y. Liu, J. Wallner, A. Bobenko, and W. Wang, *Geometry of multi-layer freeform structures for architecture*, ACM Transactions on Graphics (SIGGRAPH 2007), 26(3), Article No. 65, 2007.

[7] D. Struik, *Lectures on classical differential geometry*, Cambridge, Addison-Wesley, 1950.

[8] W. Wang, Y. Liu, D. Yan, B. Chan, R. Ling and F. Sun, *Hexagonal meshes with planar faces*, Technical Report, *TR-2008-13*, Department of Computer Science, The University of Hong Kong, 2008.